Santafé Moros, MA.; Gozálvez-Zafrilla, JM.; Lora-García, J. (2017). Experimental simulation of continuous nanofiltration processes by means of a single module in batch mode. Separation and Purification Technology. 187:233-243. doi:10.1016/j.seppur.2017.06.059

Experimental simulation of continuous nanofiltration processes by means of a single module in batch mode

Asunción Santafé-Moros, José M. Gozálvez-Zafrilla[a], Jaime Lora-García

Universitat Politècnica de València. Institute for Industrial, Radiophysical and Environmental Safety (ISIRYM). C/ Camino de Vera s/n. 46022 Valencia (Spain)

[a]Corresponding author: jmgz@iqn.upv.es

Abstract

This work proposes a method of simulating the performance of continuous nanofiltration processes by means of experimental runs performed on a laboratory set-up equipped with a spiral-wound module working in batch recirculation mode. It describes how to implement the proper changes in feed concentration and operating conditions in a batch recirculated system in order to obtain similar conditions to those of a continuous one. The analogy between the concentration process in the continuous and in the batch recirculation system is discussed and the difference in ion concentration of the cumulative permeate between the two systems is estimated numerically.

The procedure was applied in a case study to estimate the performance of a continuous process intended to remove nitrate from brackish water using a high rejection nanofiltration membrane (Dow-Filmtec NF90). The sequence of concentration steps performed in the batch-recirculated set-up yielded an estimation of the ion concentration profiles throughout the continuous system. A mathematical analysis of the results showed that the nitrate concentration in the permeate experimentally obtained in the batch system is 4.5% higher than that expected in the continuous system.

The experimental method described here can be used to design membrane system applications for which the target ions are not accurately predicted by models or are not included in commercial software.

Keywords: nanofiltration; batch mode; continuous process; process design; NF90

1. Introduction

In recent years, the nanofiltration (NF) membrane process has been shown to be a feasible solution for different water treatments including groundwater, surface water and wastewater reclamation [1-4]. NF membranes are efficient at removing divalent salts and small organic matter at low operating pressures. In addition to this general purpose, NF has increasingly been used in many new interesting environmental applications such as the removal of arsenic and persistent organic pollutants, as well as in a membrane-integrated hybrid treatment systems for desalination [5-8].

The key to using nanofiltration in these applications lies in the selection of the proper NF membrane and the design of a suitable process. The design approach is mostly influenced by the type of feed water to be processed, as well as by the permeate flow required to obtain a suitable recovery ratio to avoid excessive concentration polarization at the membrane surface. Recovery rates of 80-90% are quite common in NF applications [9].

When large feed streams are to be treated, continuous processes are usually chosen. In this case, several membrane elements are connected in series inside pressure vessels organized in stages with a different number of pressure vessels in parallel. The number of concentration stages will depend on the permeate recovery ratio and the number of membrane elements per pressure vessel.

The approach most widely used in designing a NF desalination system is to calculate permeate flow according to the net driving pressure model and to predict the passage of salts caused by the salinity gradient between feed and permeate. Computer programs have been developed by membrane manufacturers to enable the large number of calculations required in the design of NF systems.

In certain situations, the design of the continuous processes can be satisfactorily accomplished by using commercial software, for example, NF processes to treat feed compositions that fall within the range of typical desalination applications. However, commercial software may not be suitable for other feed compositions, for example in the case of ions not included in software databases.

Applying models to NF processes is limited when the model does not satisfactorily explain the mechanisms involved. Numerous papers have been written in attempts to mathematically predict the performance of NF membranes for different applications [10-16], with most of these models showing some success in a narrow range of operating parameters and feed constituents. Nevertheless, in general they are inaccurate when the feed constituents vary significantly, due to their inability to model the separation mechanism [17], e.g. when NF models are applied to desalination of brackish waters with significant ionic concentrations [18-23]. That is why Van der Bruggen et al. [2] pointed out that further modelling and simulation tools are needed and they will be the main key to the industrial implementation of nanofiltration.

When physical models cannot be applied successfully, pilot plant studies must be carried out. However, in the case of a continuous membrane process, it would not be economically feasible to experiment in a pilot plant with a large number of modules in series intended to exactly reproduce the conditions of a large process.

In considering these problems, we propose a method of using the empirical information obtained from a pilot plant with a single membrane element operated in batch-recirculated mode to experimentally simulate the performance of a continuous plant aimed at achieving a specified recovery. The use of a single module pilot plant can reduce investment and operating costs as compared to larger systems. Furthermore, smaller feed quantities are needed to perform the experiments.

A batch-recirculated process in which a membrane module is connected to a tank is typically used in the laboratory to characterize membrane behaviour by testing a

membrane element for several feed solutions under different operating conditions. In this case, both the retentate and permeate are recirculated to the tank to maintain the feed tank composition.

In a continuous membrane process, there is a gradual increase in the concentration throughout the system. If the feed and operating conditions are kept constant, the concentration profile will become stable after a short time. On the contrary, in a batch process, the system concentration continuously varies over time.

The experimental method attempts to reproduce as accurately as possible the feed and operating conditions that would exist in the continuous system to be designed. When the pressure and cross flow velocity established during the experimental procedure are similar to those of the continuous system, the same concentrations profile will be obtained and, as a consequence, similar flux and rejection.

As a case study, this experimental method is applied to estimate the performance of a continuous NF process for drinking-water production. This example was selected specifically because nanofiltration is difficult to model at significant ionic concentrations. Nanofiltration competes with reverse osmosis, being more efficient when water salinity is not very high and the main objective is to reduce hardness [24,25]. In some cases, it may also be desired to remove a specific component in addition to salt. In our case, we studied a NF membrane able to remove nitrate from water with a nitrate concentration slightly above the legal limit (50 $mg \cdot L^{-1}$). As nitrate rejection in nanofiltration is highly influenced by the presence of other ions [26-33], it is difficult to estimate the rejection results of a membrane for natural waters from results obtained with model solutions.

2. Theoretical background

In this section, the equations that determine the change in concentration due to the permeation process are obtained for a continuous process and a batch recirculated experimental set-up with a membrane module. The comparison of the expressions obtained will make it possible to analyze to what extent the permeate concentrations obtained with the experimental set-up differ from those expected for the continuous system.

2.1. Analysis of the continuous system

Figure 1 illustrates the configuration of a continuous system in which membrane modules are connected in series inside the pressure vessels. In this configuration, the concentrate of element *j*-1 becomes the feed of element *j*. For a continuous process, a mass balance can be established for a differential volume inside the membrane module (Figure 2). The differential equations representing the change in flow and concentration are:

$$\frac{\mathrm{d}Q}{\mathrm{d}A} = -J_v \tag{1}$$

$$\frac{\mathrm{d}(Q \cdot C_i)}{\mathrm{d}A} = -J_i \tag{2}$$

where subscript *i* refers to any component of the feed.

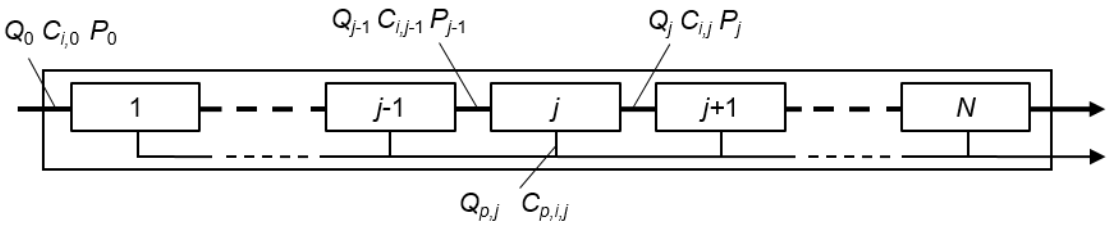

Figure 1. Diagram of continuous process with membrane elements interconnected inside the pressure vessel

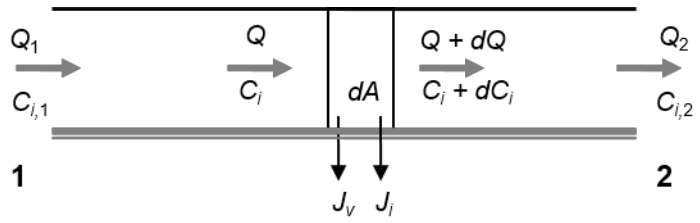

Figure 2. Membrane differential element

By dividing Eq. (2) by Eq. (1), the following expression is obtained:

$$\frac{\mathrm{d}(Q \cdot C_i)}{\mathrm{d}Q} = \frac{J_i}{J_v} = C_{p,i} \tag{3}$$

For a continuous system, the system recovery is defined in terms of volumetric flow as in Eq. (4). According to this definition and that of the rejection index *R*, the variation of the concentration with respect to the recovery is given by Eq. (5).

$$Y = \frac{Q_0 - Q}{Q_0} \tag{4}$$

$$\frac{\mathrm{d}C_i}{\mathrm{d}Y} = \frac{R_i \cdot C_i}{1 - Y} \tag{5}$$

In general, the rejection index depends on concentration and operating conditions, and thus varies throughout the membrane system. In our approach, an average value is assumed for each module at each position *j*. Under this simplification, Eq. (5) can be integrated from the conditions of the entering stream to the exiting stream of the module at position *j*, leading to a concentration ratio between the two streams as follows:

$$\left(\frac{C_{i,j}}{C_{i,j-1}}\right)_{cont} = \left(\frac{1-Y_j}{1-Y_{j-1}}\right)^{-R_{i,j}}$$

(6)

In the latter equation, the right-hand term can be expressed in terms of module recovery *y*.

$$\frac{1-Y_j}{1-Y_{j-1}} = \frac{Q_j}{Q_{j-1}} = 1-y_j$$

(7)

The successive application of Eq. (6) from the first module up to a module in position *n* leads to the ratio of the concentration of the exiting stream from module *n* to the concentration of the input stream to the system (Eq. 8).

$$\left(\frac{C_{i,n}}{C_{i,0}}\right)_{cont} = \prod_{j=1}^{n}\left(1-y_j\right)^{-R_{i,j}}$$

(8)

The system recovery achieved after module *n* can be obtained by mass balance, neglecting density effects:

$$Y_n = 1-\prod_{j=1}^{n}\left(1-y_j\right)$$

(9)

Therefore, a component balance taking into account Eqs. (8) and (9) leads to a concentration of the permeate stream obtained by mixing the permeate streams of the modules up to position *n* for the continuous system:

$$\left(\frac{\bar{C}_{p,i,n}}{C_{i,0}}\right)_{cont} = \frac{1-\prod_{j=1}^{n}\left(1-y_j\right)^{1-R_{i,j}}}{1-\prod_{j=1}^{n}\left(1-y_j\right)}$$

(10)

2.2. Analysis of the batch recirculated system

A pilot plant with a single spiral-wound element can be used to estimate the performance of the continuous system thanks to the partial analogy existing between the two systems.

The performance of each of the individual elements in the continuous system can be simulated experimentally by means of a batch recirculated system using a sequence of two phases: the first to ensure the stabilization of permselective results, and the second to concentrate the feed tank solution so as to achieve the input conditions corresponding to the next element of the membrane array.

In the stabilization phase, the plant works in the total batch recirculation mode; i. e., both permeate and retentate are recycled back to the feed tank (Figure 3a). The purpose of this phase is to get close to steady-state conditions. Because of the short residence time of the liquid inside the module, changes in the operating conditions inside the module can be considered instantaneous in practice. However, a significant period of time is usually required for the membrane to adapt completely to the new operating conditions.

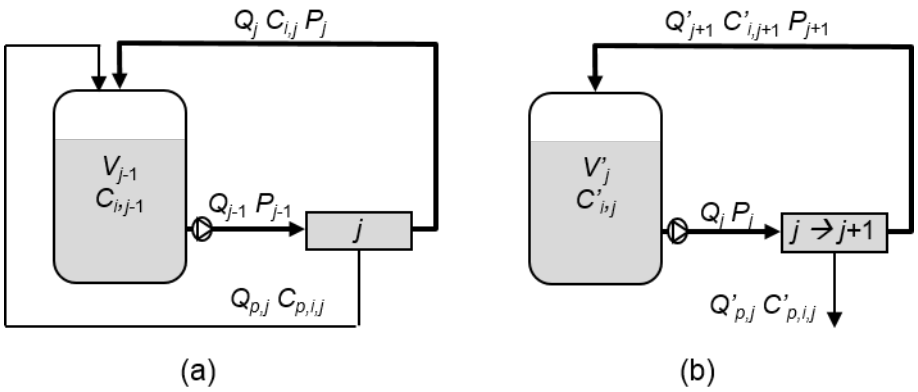

Figure 3. Phases of the experimental simulation in the batch system: a) stabilization using the total recirculation, b) feed concentration. Variables with prime evolve due to the change of feed concentration at the new flow and input pressure.

Once the stationary state for the simulation of the module corresponding to the position *j* in the continuous system has been achieved, the operating conditions are changed to those of the input of the following module in the series (*j*+1). The change of feed pressure and input flow can easily be set if a speed-variable volumetric pump is used. The change in concentration could be carried out by replacing the feed solution with another with the required concentration ($C_{i,n+1}$). Nevertheless, this way of working is time-consuming and difficult to carry out for solutions containing multiple ions. Another more practical possibility is to use the same membrane to concentrate the tank solution by withdrawing a certain amount of permeate (Figure 3b).

During the permeation process, the differential equations for total mass balance and component balance applied to the batch system relate the variations of volume and component in the feed tank with the permeation through a membrane of finite area:

$$\frac{\mathrm{d}V}{\mathrm{d}t} = -J_{v,m} \cdot A_m \tag{11}$$

$$\frac{\mathrm{d}(V \cdot C_i)}{\mathrm{d}t} = -J_{i,m} \cdot A_m \tag{12}$$

By dividing Eq. (12) by Eq. (11), the following expression is obtained:

$$\frac{\mathrm{d}(V \cdot C_i)}{\mathrm{d}V} = \frac{J_{i,m}}{J_{v,m}} = C_{p,i,m} \tag{13}$$

If the system recovery for the batch system is defined as a function of the tank volume (Eq. 14), the variation of the concentration with respect to the recovery is obtained in Eq. (15)

$$Y = \frac{V_0 - V}{V_0} \tag{14}$$

$$\frac{\mathrm{d}C_i}{\mathrm{d}Y} = \frac{R_{m,i} \cdot C_{i,m}}{1 - Y} \tag{15}$$

In the case of a plate-and-frame module equipped with a flat sheet membrane of very small membrane area, the module rejection coincides with the membrane rejection.

It can be seen that Eq. (15) is formally equal to Eq. (5), which implies that it is theoretically possible to exactly match the behavior of the continuous system with the batch system if identical operating conditions (pressure, temperature, concentration and flow) are used at each level of recovery. However, this can be difficult to achieve because the hydrodynamic conditions in the plate-and-frame module can differ from those existing in the spiral-wound module, thereby affecting concentration polarization and consequently mass transfer through the membrane. The use of a spiral-wound module in the batch recirculation system would give a better approximation of the operating conditions of the continuous process and additionally in estimating the pressure profile throughout the system.

If a spiral-wound membrane module is used, the permeate is formed by the contribution of the differential area elements of the module. Consequently, the module rejection can be better expressed in terms of the module recovery and an average local membrane rejection in the module.

$$R_m(y,R) = 1 - \frac{1-(1-y)^{1-R}}{y}$$

(16)

In this case, the analogy with Eq. (5) is not exact. Significant recovery per module implies that the values of module rejection and local rejection can differ significantly.

The integration of Eq. (15) between the system recovery values corresponding to the input and the output of a module yields:

$$\left(\frac{C_{i,j}}{C_{i,j-1}}\right)_{batch} = \left(\frac{1-Y_j}{1-Y_{j-1}}\right)^{-R_m(y_j,R_i)}$$

(17)

Consequently, using the same analysis as for the continuous case, the concentration of the batch system's accumulated permeate is obtained:

$$\left(\frac{\bar{C}_{p,i,n}}{C_{i,0}}\right)_{batch} = \frac{1-\prod_{j=1}^{n}(1-y_j)^{1-R_m(y_j,R_{i,j})}}{1-\prod_{j=1}^{n}(1-y_j)}$$

(18)

Note, that the latter equation can be applied even if volume samples from the tank are withdrawn for analysis because the calculation is based on module recoveries instead of system recoveries.

2.3. Estimation of the difference in permeate concentration between the two systems

Applying Eqs. (10) and (18) to experimental values of module rejection and recovery obtained with the batch system gives an estimation of the relative difference between the accumulated permeate of the batch and the permeate produced by the continuous system (Eq. 19). Note that the average membrane rejection is estimated from module rejection by Eq. (16).

$$\epsilon_n = \frac{\prod_{j=1}^{n}(1-y_j)^{1-R(y_j,R_{m,i,j})} - \prod_{j=1}^{n}(1-y_j)^{1-R_{m,i,j}}}{1-\prod_{j=1}^{n}(1-y_j)^{1-R(y_j,R_{m,i,j})}}$$

(19)

Figure 4 shows the relative difference in permeate concentration for several ideal situations with constant module recovery and a constant rejection index for a generic component. Given a system recovery, the relative difference in permeate concentration is smaller if modules with smaller recovery are used. The greater number of modules required implies that the solution approaches that of the continuous system. It can also be seen that the greater the rejection index, the greater the relative difference. For this special case, there is a mathematical limit for the relative difference at total rejection (Eq.

20) in spite of the absolute difference tending to zero as rejection increases. In Figure 4, the values of relative difference of permeate concentration for the rejection index of 99% practically coincide with those predicted by Eq. (20).

$$\epsilon_{(R=100\%)} = -1 - \frac{\ln(1-y)}{y} \tag{20}$$

It can also be seen that, given the rejection and recovery of the individual modules, the relative difference in permeate concentration slightly decreases as the system recovery increases.

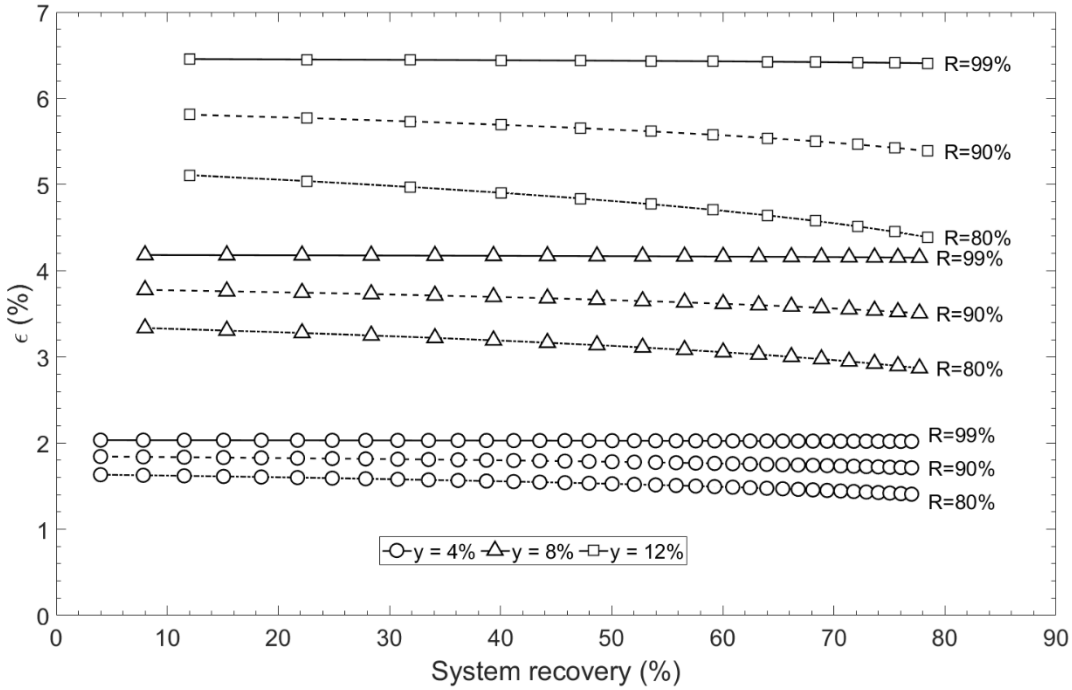

Figure 4. Relative difference in permeate concentration between the batch system and the continuous system as a function of membrane rejection (*R*) and module recovery (*y*)

3. Experimental simulation procedure

It has been noted that, to simulate the performance of the elements connected in series inside a pressure vessel housing, the membrane module must be exposed to similar operating conditions to those expected for the continuous system (feed concentration, feed flow and applied pressure).

During the experimental runs, the operating conditions related to the module in position *n* are fixed and the pilot plant works in a total recirculation loop (permeate and concentrate streams are recycled back to the feed tank). The experiments must be continued until stabilization of the permeate flow and permeate conductivity is attained.

Once stabilization is achieved, sample volumes (V^s) are collected from the feed tank and the permeate stream to obtain their conductivity, pH and ionic composition.

To achieve the operating conditions corresponding to the module in the next position of the continuous system, *n*+1, the following procedure is followed:

i) Input pressure is set at the retentate pressure of the preceding module in position *n*.

ii) Feed flow is set at the retentate flow of the preceding module in position *n*.

iii) The permeate volume required to reach the ionic concentration for the module *n*+1 in the feed tank is removed.

According to the previously discussed analogy between the continuous and the batch recirculated systems, the volume of the feed tank must be reduced by removing the permeate volume by the same ratio as the flow reduction in the element of the continuous system (Eq. 12). In addition, the volume of feed sample removed for analysis must be taken into account. Applying these conditions to the transition from the element in position *n* to the one in position *n*+1, yields:

$$\frac{(V_{n-1} - V^s) - V_n}{(V_{n-1} - V^s)} = \frac{Q_{n-1} - Q_n}{Q_{n-1}} \tag{21}$$

Therefore, to achieve the new conditions corresponding to module *n*+1, the volume of permeate to be withdrawn during the concentration phase is:

$$\Delta V_{p,n\to n+1} = (V_{n-1} - V^s) \cdot \frac{Q_{n-1} - Q_n}{Q_{n-1}} \tag{22}$$

The permeate volume is removed by interrupting the recirculation and withdrawing quantities evenly spaced over one hour to help membrane stabilization.

To simulate the first membrane stage of the continuous system, the above procedure is repeated for each module contained in the pressure vessel.

When the previously specified number of modules of one stage has been simulated, it is necessary to take into account that the number of pressure vessels in parallel in the next stage is smaller to set the flow entering to the pressure vessels to a higher, suitable value. On the other hand, a booster pump can be used between stages. In this case, the input pressure used in the first experimental run of the new stage must be increased to simulate the effect of the pump in the continuous system.

4. Case study

The experimental simulation was applied in a case study to estimate the performance of a nanofiltration plant treating tap water containing nitrate ions slightly exceeding the

concentration limit for drinking water (50 $mg \cdot L^{-1}$). The ionic composition of the feed water is shown in Table 1.

Table 1. Feed water composition

Ions	Concentration ($mg \cdot L^{-1}$)
Cl^-	97.38
SO_4^{2-}	106.09
NO_3^-	68.26
CO_3^{2-}	0.54
HCO_3^-	212.13
Na^+	25.29
K^+	1.76
Mg^{2+}	32.48
Ca^{2+}	114.95
TDS	659 mg/L
pH	7.48

The NF90-2540 spiral-wound membrane (Dow-Filmtec) was selected for the study as the feed water slightly exceeded the nitrate ion concentration and its manufacturers included nitrate removal as a feasible application for this membrane. The experimental setup was a pilot plant with a single spiral-wound module described in a previous study [34]. The flow-meter of the pilot plant used is placed at the retentate stream. Therefore, to achieve the objective values of the feed pressure and feed flow, the permeate flow was measured and the retentate flow was modified by operating the volumetric pump and the retentate valves until the sum of both flows is stabilized.

Taking into account the low salinity of the feed water, a target system recovery rate of 80% was established. The number of 6 modules per pressure vessel was arbitrarily chosen for each stage.

The initial operating conditions that correspond to the experimental simulation of the first stage's first membrane element are shown in Table 2. The input flow and the input pressure used in the study ensured that the first module of the system did not fail to keep within the limiting operating conditions established by the manufacturer. The initial feed volume of the pilot plant included those of the tank and pipes. The initial pH of the feed was adjusted using hydrochloric acid to have an expected LSI value of zero in the final concentrate at the target system recovery rate. The temperature of the tank was kept at 20 °C throughout the experiments.

Table 2. Initial operating conditions and initial feed conditions

Applied input pressure (MPa)	0.65
Input flow ($m^3 \cdot h^{-1}$)	0.75
Volume (L)	53.12
Adjusted pH	6.2

The experimental runs were carried out for at least two hours. After this time, the criterion for the membrane stabilization performance was that the flow and conductometry of the permeate should differ by less than 0.5% between measurements separated by 1 hour. The volume samples taken from the feed tank and the permeate stream for complete analysis were V^s = 0.125 L. Anion and cation concentrations in both feed and permeate were analyzed using a 790P Metrohm ion chromatograph. Metrosep A Supp 5 and Metrosep C2 (Metrohm) columns were used for anions and cations respectively.

For the first simulation step of each membrane stage, the input flow and the input pressure were set to the initial values defined in Table 2, as the use of booster pumps between stages was considered.

5. Results and discussion

5.1. Operating conditions

Table 3 shows the flow, pressure and total ionic concentration (as total dissolved solids) for the feed and the permeate stream obtained for each of the membrane elements simulated experimentally. Note the small flow balance errors for each simulated module, which are a consequence of the precision of the flow-meter. The accumulated effect of these errors on the flow balance for each stage was less than 4.5%, 3.9% and 0.9% respectively. As can be seen, the experimental procedure determined that three stages were necessary to achieve the target recovery for the membrane used and the feed treated.

Table 3. Experimental results: Flow, total dissolved solids and pressure for feed and permeate streams

Stage number	Element number	Feed flow (m^3/h)	TDS (mg/L)	Pressure MPa	Permeate flow (m^3/h)	TDS (mg/L)	y (%)	Y (%)
1	1	0.761	578.5	0.64	0.092	10.97	12.0	12.1
	2	0.656	664.4	0.57	0.077	12.25	11.7	22.4
	3	0.582	733.4	0.50	0.062	16.04	10.7	30.7
	4	0.520	811.9	0.45	0.050	17.60	9.6	37.3
	5	0.470	897.5	0.40	0.045	22.49	9.6	43.3
	6	0.418	985.5	0.35	0.039	24.85	9.3	48.6
2	7	0.750	1074.2	0.65	0.081	17.25	10.7	54.2
	8	0.660	1187.9	0.56	0.070	20.03	10.5	59.0
	9	0.585	1341.8	0.50	0.055	25.48	9.5	62.9
	10	0.528	1446.0	0.46	0.049	30.70	9.2	66.3
	11	0.481	1554.7	0.41	0.036	34.88	7.5	68.9
	12	0.443	1679.1	0.36	0.033	48.77	7.5	71.2
3	13	0.752	1836.2	0.65	0.072	30.39	9.6	73.9
	14	0.681	1997.2	0.57	0.061	33.87	9.0	76.3
	15	0.619	2192.4	0.51	0.049	42.97	7.9	78.1
	16	0.567	2361.1	0.45	0.037	57.39	6.6	79.1
	17	0.532	2474.1	0.40	0.033	65.48	6.2	80.8
	18	0.504	2637.2	0.34	0.024	84.26	4.8	81.8

For each simulated stage, the flows of the initial feed and that of the final concentrate correspond to those of any of the parallel vessels of the continuous system. Therefore, the number of pressure vessels can be calculated as indicated in Figure 5. From the results shown in Table 3, the ratio of the number of pressure vessels of the second stage and third stage to the number of pressure vessels of the first stage were 0.53 and 0.30 respectively. The specific number of pressure vessels depends on the feed flow treated by the system.

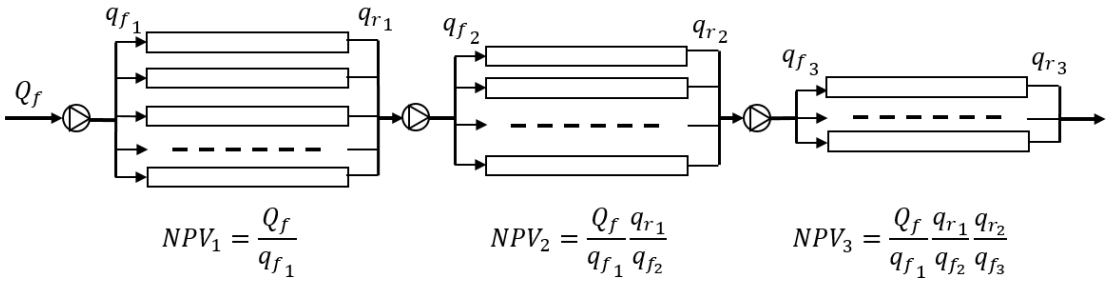

Figure 5. Configuration of the continuous system (NPV_i = number of pressure vessels, Q_f = feed flow of the system, $q_{f,i}$,$q_{r,i}$ = feed and retentate flow per parallel vessel at stage i)

5.2 Evolution of permeate flux throughout the system

Figure 6 shows the decrease in the permeate flux as a function of the module position in each stage of the system. The observed decrease in flux is a consequence of both the decrease in the effective pressure caused by the pressure drop and the increase in the osmotic pressure due to the concentration rise. In this case, the osmotic pressure increased from 0.03 MPa for the initial feed solution to 0.14 MPa for the final concentrate.

It can be noticed that despite having restored the feed pressure between stages, the value of the permeate flux did not reach the level of the first module of the first stage owing to the concentration increase through the process.

As can be seen in Figure 7, the permeate flux and the effective pressure, calculated using bulk concentrations, fit well to a straight line for each stage. As the slope values obtained are very close, the effect of concentration polarization is low [28, 35].

The average specific flux of the system (normalized to 25 ºC) was 1.63×10^{-5} $m^3 \cdot m^{-2} \cdot s^{-1} \cdot MPa^{-1}$. This value is close to those calculated from the results obtained by others authors treating saline waters with the NF90 (1.23×10^{-5} – 1.89×10^{-5} $m^3 \cdot m^{-2} \cdot s^{-1} \cdot MPa^{-1}$) [5,36-38].

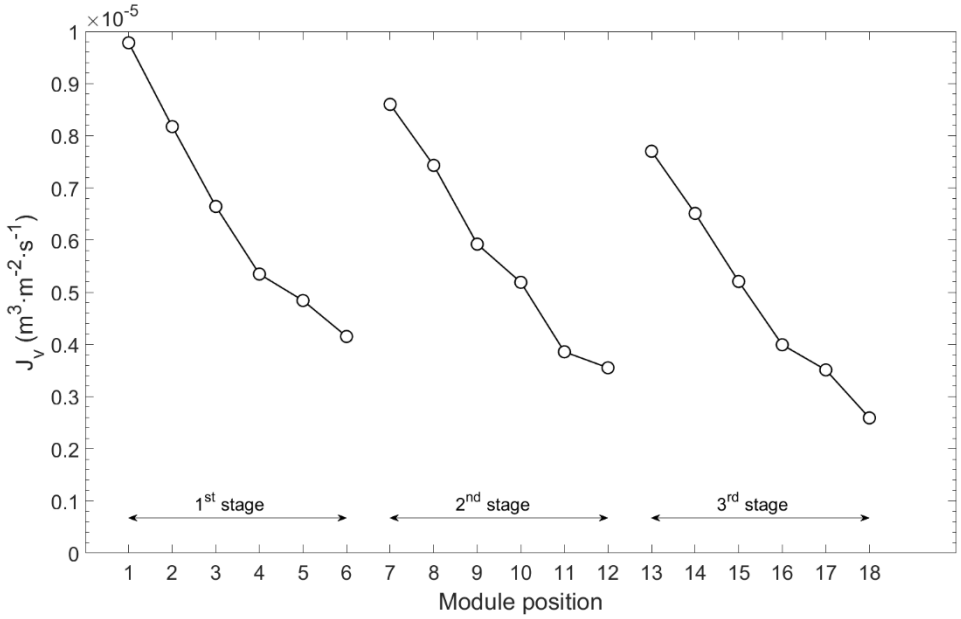

Figure 6. Permeate flux at each module position simulated experimentally

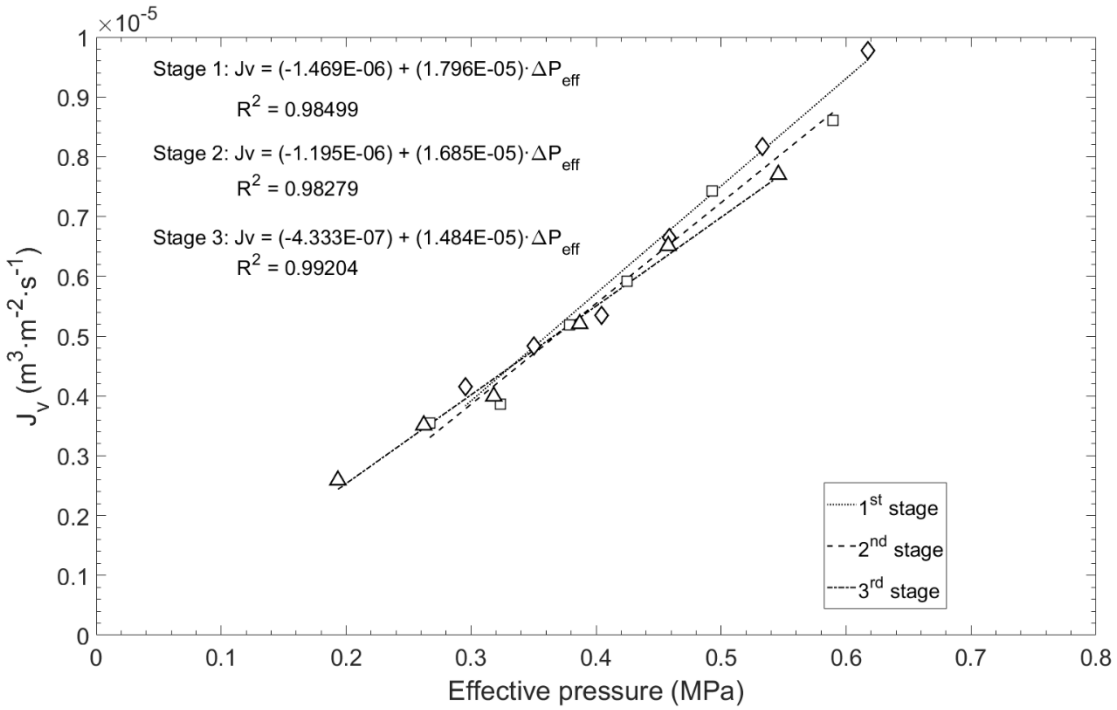

Figure 7. Permeate flux vs effective pressure of each membrane module simulated experimentally. Linear regressions calculated for each stage.

5.3. Evolution of ion rejection throughout the system

Table 4 summarizes the expected ionic composition for the exiting concentrate of each stage, the average ionic concentrations for the permeate of each stage and for the system. For each stage, the average ionic concentration of the permeate stream was

calculated using the values of the permeate concentrations and the flow of each of the modules. In this case, the process was able to reject 95% of the total dissolved solids.

Moreover, in the case studied, the nitrate ion rejection was high enough to achieve a suitable permeate quality for drinking water (< 50 mg/L). Process configurations of two and three stages to obtain a system recovery of nearly 80% were simulated using the Filmtec® Reverse Osmosis System Analysis software (ROSA 9.1). In general, the evaluated configurations reported ion concentrations in the total permeate that were higher than those obtained using the experimental procedure. Redondo & Lanari [39] also reported higher ion rejections than those predicted for sodium, bicarbonate, chloride and sulfate in a water treatment plant. The highest differences were obtained for the divalent ions (until 80% of relative difference), probably because of their low concentration in the permeate (less than 1 mg/L). For the monovalent ions, sodium and chloride the relative difference was 25% and 6% respectively. It is remarkable that nitrate concentrations predicted by the software fell in the range of 30 – 40 mg/L, whereas the experimental value obtained was 11.40 mg/L. The latter result shows the usefulness of the experimental procedure in this type of situation.

Table 4. Ionic composition of the system's streams ($mg \cdot L^{-1}$)

Component	Adjusted Feed	Concentrate			Permeate			Total permeate
		1st	2nd	3rd	1st	2nd	3rd	
K^+	1.76	3.40	5.53	7.87	0.41	0.66	1.40	0.78
Na^+	25.29	45.64	74.42	103.84	4.02	6.71	12.36	7.31
Mg^{2+}	32.48	61.96	107.70	155.09	0.23	0.27	0.36	0.28
Ca^{2+}	114.95	209.97	357.96	531.90	0.43	0.72	1.10	0.72
HCO_3^-	40.10	70.00	110.00	167.96	1.05	0.93	1.35	1.10
NO_3^-	68.26	123.27	204.20	303.27	6.43	10.96	18.46	11.40
Cl^-	189.55	366.71	650.77	1006.31	3.28	6.24	11.79	6.71
SO_4^{2-}	106.09	193.23	325.57	489.94	0.05	0.15	0.27	0.15
TDS	578.48	1074.20	1836.20	2766.18	15.89	26.60	47.10	28.43
pH	6.20	6.29	6.19	6.56	5.55	5.61	5.66	5.60

Figures 8 and 9 show the rejection of divalent and monovalent ions, respectively. The ion rejection for sulfate is quite greater than that of monovalent anions what is in keeping with a negatively charged membrane. As reported by others researchers, this membrane exhibits an isoelectric point around 4.0 - 5.0 [33,40-43], so, for the operating pH, around 6.2, the membrane is expected to be negatively charged. High ionic rejections, not only for divalent ions but also for monovalent ones, have also been obtained in other studies developed with the NF90 membrane treating real seawater [44], water from a natural gas production site [45], groundwater [46] and ionic complex solution [28]. The rejection of divalent ions (SO_4^{2-}, Ca^{2+}, Mg^{2+}) was not very dependent on the concentration. However, the rejection of monovalent cations fell significantly at each stage, especially in stages 2 and 3. In the case of the monovalent anions, both chloride and nitrate ions showed similar profiles in each stage. The rejection of ion chloride was high (over 99%) and nitrate rejection was over 90% in all stages. The greater rejection for chloride anion compared to that of the nitrate ion has been reported not only for this membrane [28, 46] but also for other NF membranes [47,48]. These authors attribute this behavior to their different hydration energy.

In general, ion rejection decreased throughout the stage due to the decrease in volumetric flux, which in turn is caused by the pressure drop and to a lesser extent by the concentration increase. This is confirmed by the fact that on resetting the pressure value at the beginning of stages 2 and 3 to the value of the feed input to the system, the rejection index is largely recovered for most ions.

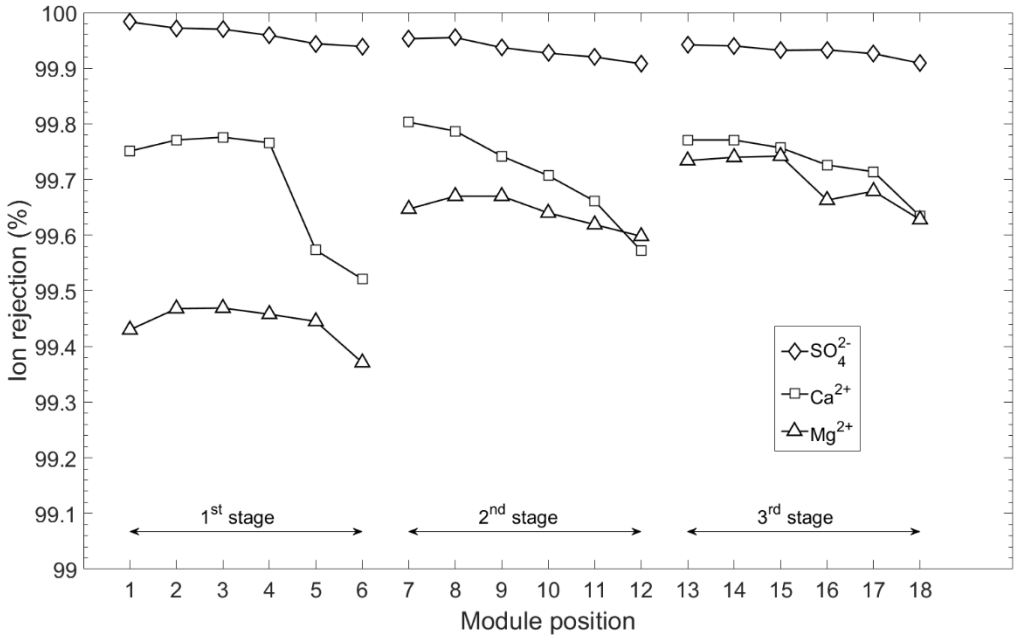

Figure 8. Divalent ion rejection corresponding to each membrane module position simulated experimentally

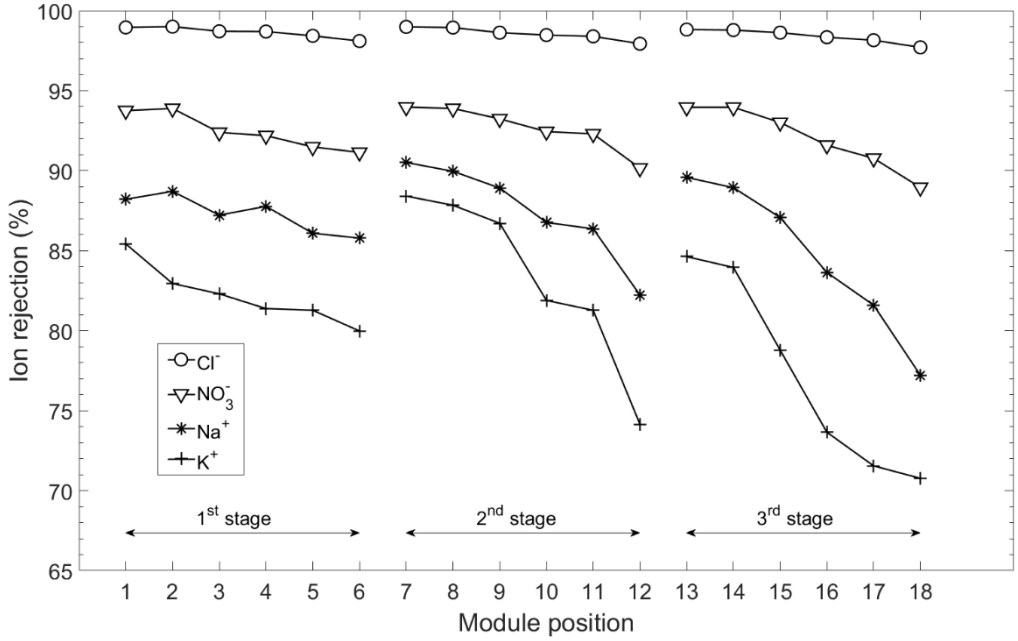

Figure 9. Monovalent ion rejection corresponding to each membrane module position simulated experimentally

5.4 System performance

For each of the experimental runs carried out, the volume reduction factor (VRF) achieved in the feed tank and the concentration factor (CF) were calculated from the initial values of the volume and the total dissolved solids in the feed tank:

$$VRF_n = \frac{V_0}{V_n} \tag{23}$$

$$CF_n = \frac{TDS_n}{TDS_0} \tag{24}$$

In Figure 10, it can be seen that the CF and VRF plots versus the module position do not overlap and that the gap between the two curves slightly increases with concentration, although this effect is not striking because of the high ionic rejection of the NF90 membrane.

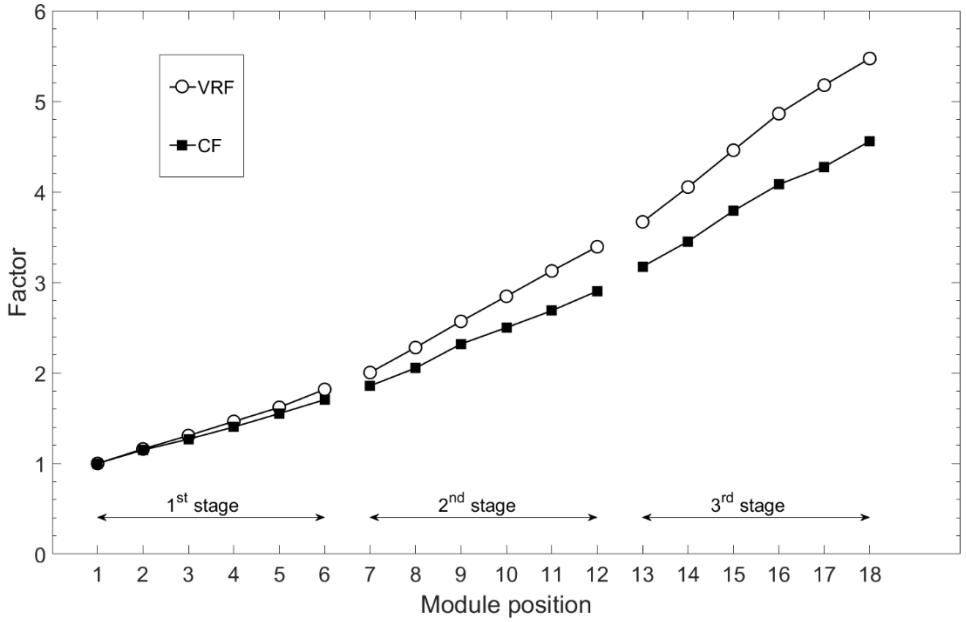

Figure 10. Volume reduction factor and concentration factor obtained in the experimental simulation of the different module positions

5.5. Estimation of the relative difference in permeate concentration

To estimate the relative difference in permeate concentration obtained in the experimental procedure, Eq. (19) was applied to each of the experimental module recoveries obtained (Table 3) and the ion rejection results. The results for each ion are shown as a function of the system recovery in Figure 11. It can be seen that, with a system recovery of less than 80%, the relative difference in rejection for all ions is between 3 and 7% and that it is higher the more the ion is rejected. In fact, ions rejected

over 98% show practically the same values of relative difference in permeate concentration. In the case of nitrate, this relative difference was 4.5% for the final recovery, which implies that the nitrate rejection of the continuous system will be slightly better than the one directly predicted in the experimental procedure with the batch system.

Compared with the ideal case of constant module recovery (Figure 4), it can be seen that the relative difference in permeate concentration falls more sharply as the system recovery increases. This is a consequence of the smaller module recovery caused by the decrease of the driving force as the total ionic concentration is increased.

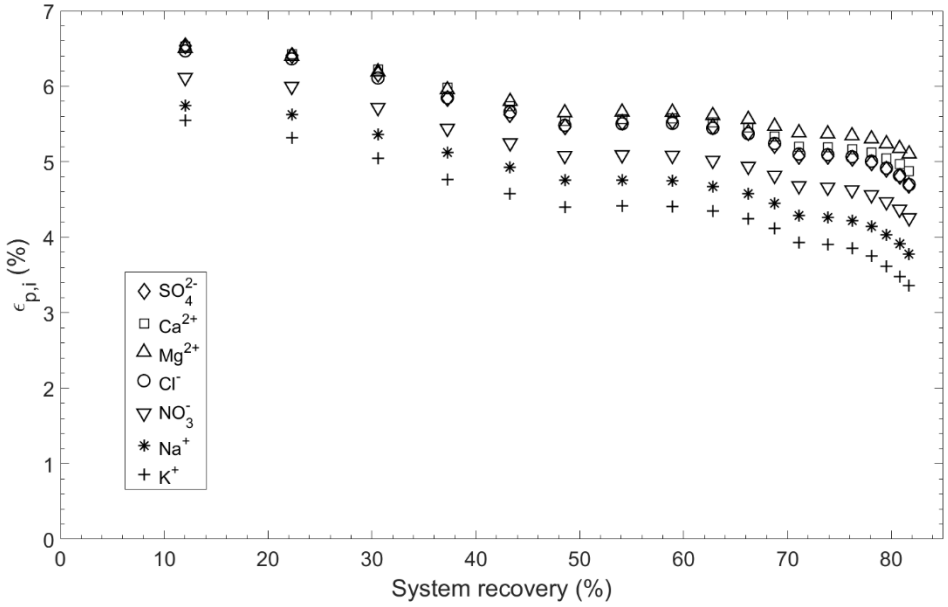

Figure 11. Relative difference between the permeate concentration in the batch system simulation and the permeate concentration expected in the continuous system.

Conclusions

This paper shows an experimental procedure to estimate the performance of a continuous system from an experimental set-up based on the use of a module and a tank working in the batch recirculation mode. The method used to change concentration and operating conditions is described to obtain results as near as possible to those expected for the continuous system. The use of a commercial module instead of a small-area plate-and-frame module gives a better approximation to the pressure drop that it would occur in the continuous plant. However, as a commercial module has a significant recovery, the concentration of the accumulated permeate obtained by a batch system differs from the permeate concentration that would be obtained by a continuous system.

We also obtained expressions to estimate the relative difference of permeate concentrations between the batch and continuous systems. It was determined that the relative difference in permeate concentration depends on module recovery and ion rejection. The higher the module recovery in the experimental procedure, the higher the relative difference in concentration between the two systems. Furthermore, this relative

difference is higher at a higher ion rejection, with a theoretical limit for highly rejected ions. For example, using a module at 15% recovery, the maximum relative difference obtained for highly rejected ions would be 8.3%, and below this value for the less rejected ions. It can therefore be said that the experimental simulation procedure using a single module is accurate enough for many situations.

The methodology was applied in a case study to a nanofiltration process intended to produce drinking water from brackish water. The estimated relative difference in permeate concentration was found to be in the range of 3-6.5%. In the case of the nitrate ion, whose rejection is not well predicted by transport models, the difference was 4.5%.

The proposed experimental method can thus be used to design membrane systems applications for which the target ions, such as nitrates, are not accurately predicted by models, or are not included in commercial software databases, such as heavy metals. We propose implementing the initial design using the commercial software by including the main ions in order to determine the operating conditions of the system. Afterwards, the proposed experimental method can be used to validate or improve the estimation of the target ion rejection. The information obtained can also be used to adjust the final design of the continuous system.

List of symbols

A membrane area from the inlet to the continuous system to a specific position, m^2

C concentration of the streams from feed to retentate, $mg \cdot L^{-1}$

C_p concentration of the permeate stream, $mg \cdot L^{-1}$

CF concentration increase factor

J_i flux of component, $mg \cdot m^{-2} \cdot s^{-1}$

J_v volumetric flux, $m^3 \cdot m^{-2} \cdot s^{-1}$

NPV_i Number of parallel pressure vessels of stage i

P pressure applied, MPa

Q flow of streams from feed to retentate, $m^3 \cdot h^{-1}$

Q_p flow of permeate stream, $m^3 \cdot h^{-1}$

R local membrane rejection in a differential or average local membrane rejection for a module

t time, h

TDS total dissolved solids, $mg \cdot L^{-1}$

V volume of solution in the feed tank of the batch system, L

V^s volume of samples removed from the feed tank for analysis, L

VRF volume reduction factor

y module recovery

Y system recovery

ε relative difference

Subscripts

batch batch system

cont continuous system

i component

j module position

m property in the spiral-wound module of the experimental set-up

n module position

0 property in the feed stream or in the feed tank

Superscripts

‘ prime is applied to variables changing in the concentration process after setting new operating conditions

Acknowledgements

This work was supported by the Spanish Ministry for Economy and Competitiveness [Project OPTIMEM CTM2010-20248].

References

[1] A.W. Mohammad, Y.H. Teow, W.L. Ang, Y.T. Chung, D.L. Oatley-Radcliffe, N. Hilal, Nanofiltration membranes review: Recent advances and future prospects, Desalination. 356 (2015) 226–254. doi:10.1016/j.desal.2014.10.043.

[2] B. Van der Bruggen, M. Mänttäri, M. Nyström, Drawbacks of applying nanofiltration and how to avoid them: A review, Sep. Purif. Technol. 63 (2008) 251–263. doi:10.1016/j.seppur.2008.05.010.

[3] N. Hilal, H. Al-Zoubi, N.A. Darwish, A.W. Mohamma, M. Abu Arabi, A comprehensive review of nanofiltration membranes:Treatment, pretreatment,

modelling, and atomic force microscopy, Desalination. 170 (2004) 281–308. doi:10.1016/j.desal.2004.01.007.

[4] A.I. Schäfer, A.G. Fane, T.D. Waite, eds., Nanofiltration. Principles and Applications, Elsevier Advanced Technology, Kidlington, UK, 2005.

[5] M. Pontié, H. Dach, J. Leparc, M. Hafsi, A. Lhassani, Novel approach combining physico-chemical characterizations and mass transfer modelling of nanofiltration and low pressure reverse osmosis membranes for brackish water desalination intensification, Desalination. 221 (2008) 174–191. doi:10.1016/j.desal.2007.01.075.

[6] M. Sen, A. Manna, P. Pal, Removal of arsenic from contaminated groundwater by membrane-integrated hybrid treatment system, J. Memb. Sci. 354 (2010) 108–113. doi:10.1016/j.memsci.2010.02.063.

[7] B. Van der Bruggen, C. Vandecasteele, Removal of pollutants from surface water and groundwater by nanofiltration: overview of possible applications in the drinking water industry, Environ. Pollut. 122 (2003) 435–445. doi:10.1016/S0269-7491(02)00308-1.

[8] J. Radjenović, M. Petrović, F. Ventura, D. Barceló, Rejection of pharmaceuticals in nanofiltration and reverse osmosis membrane drinking water treatment, Water Res. 42 (2008) 3601–3610. doi:10.1016/j.watres.2008.05.020.

[9] M.S. Mohsen, J.O. Jaber, M.D. Afonso, Desalination of brackish water by nanofiltration and reverse osmosis, Desalination. 157 (2003). doi:10.1016/S0011-9164(03)00397-7.

[10] E.R. Cornelissen, J. Verdouw, A.J. Gijsbertsen-Abrahamse, J.A.M.H. Hofman, A nanofiltration retention model for trace contaminants in drinking water sources, Desalination. 178 (2005) 179–192. doi:10.1016/j.desal.2004.11.047.

[11] J. Kheriji, B. Hamrouni, Boron removal from brackish water by reverse osmosis and nanofiltration membranes: application of Spiegler-Kedem model and optimization, Water Sci. Technol. Water Supply. 16 (2016) 684–694.

[12] V. Yangali-Quintanilla, A. Sadmani, M. McConville, M. Kennedy, G. Amy, A QSAR model for predicting rejection of emerging contaminants (pharmaceuticals, endocrine disruptors) by nanofiltration membranes, Water Res. 44 (2010) 373–384. doi:10.1016/j.watres.2009.06.054.

[13] S. Darvishmanesh, A. Buekenhoudt, J. Degrève, B. Van der Bruggen, Coupled series–parallel resistance model for transport of solvent through inorganic nanofiltration membranes, Sep. Purif. Technol. 70 (2009) 46–52. doi:10.1016/j.seppur.2009.08.011.

[14] J. Geens, K. Boussu, C. Vandecasteele, B. Van der Bruggen, Modelling of solute transport in non-aqueous nanofiltration, J. Memb. Sci. 281 (2006) 139–148. doi:10.1016/j.memsci.2006.03.028.

[15] X.-L. Wang, W.-J. Shang, D.-X. Wang, L. Wu, C.-H. Tu, Characterization and applications of nanofiltration membranes: State of the art, Desalination. 236 (2009) 316–326. doi:10.1016/j.desal.2007.10.082.

[16] W.R. Bowen, J.S. Welfoot, Modelling the performance of membrane nanofiltration—critical assessment and model development, Chem. Eng. Sci. 57 (2002) 1121–1137. doi:10.1016/S0009-2509(01)00413-4.

[17] M. Wilf et al., The Guidebook to Membrane Desalination Technology, Balaban Desalination Publications, L'Aquila, Italy, 2007.

[18] C. Labbez, P. Fievet, A. Szymczyk, A. Vidonne, A. Foissy, J. Pagetti, Retention of mineral salts by a polyamide nanofiltration membrane, Sep. Purif. Technol. 30 (2003) 47–55. doi:10.1016/S1383-5866(02)00107-7.

[19] A.I. Cavaco Morão, A. Szymczyk, P. Fievet, A.M. Brites Alves, Modelling the separation by nanofiltration of a multi-ionic solution relevant to an industrial process, J. Memb. Sci. 322 (2008) 320–330. doi:10.1016/j.memsci.2008.06.003.

[20] V. Silva, V. Geraldes, A.M. Brites Alves, L. Palacio, P. Prádanos, A. Hernández, Multi-ionic nanofiltration of highly concentrated salt mixtures in the seawater range, Desalination. 277 (2011) 29–39. doi:10.1016/j.desal.2011.03.088.

[21] S. Déon, A. Escoda, P. Fievet, R. Salut, Prediction of single salt rejection by NF membranes: An experimental methodology to assess physical parameters from membrane and streaming potentials, Desalination. 315 (2013) 37–45. doi:10.1016/j.desal.2012.09.005.

[22] S. Déon, A. Escoda, P. Fievet, P. Dutournié, P. Bourseau, How to use a multi-ionic transport model to fully predict rejection of mineral salts by nanofiltration membranes, Chem. Eng. J. 189-190 (2012) 24–31. doi:10.1016/j.cej.2012.02.014.

[23] D.L. Oatley-Radcliffe, S.R. Williams, M.S. Barrow, P.M. Williams, Critical appraisal of current nanofiltration modelling strategies for seawater desalination and further insights on dielectric exclusion, Desalination. 343 (2014) 154–161. doi:10.1016/j.desal.2013.10.001.

[24] E. Wittmann, T. Thorsen, Water Treatment, in: A.I. Schäfer, A.G. Fane, T.D. Waite (Eds.), Nanofiltration. Principles and Applications, Elsevier Advanced Technology, Kidlington, UK, 2005: pp. 120–146.

[25] F. Elazhar, J. Touir, M. Elazhar, Techno-economic comparison of reverse osmosis and nanofiltration in desalination of a Moroccan brackish groundwater, Desalin. Water Treat. 55 (2015) 2471–2477.

[26] S. Choi, Z. Yun, S. Hong, K. Ahn, The effect of co-existing ions and surface characteristics of nanomembranes on the removal of nitrate and fluoride, Desalination. 133 (2001) 53–64. doi:10.1016/S0011-9164(01)00082-0.

[27] L. Paugam, S. Taha, G. Dorange, P. Jaouen, F. Quéméneur, Mechanism of nitrate ions transfer in nanofiltration depending on pressure, pH, concentration and medium composition, J. Memb. Sci. 231 (2004) 37–46. doi:10.1016/j.memsci.2003.11.003.

[28] F. Garcia, D. Ciceron, A. Saboni, S. Alexandrova, Nitrate ions elimination from drinking water by nanofiltration: Membrane choice, Sep. Purif. Technol. 52 (2006) 196–200. doi:10.1016/j.seppur.2006.03.023.

[29] I. Musbah, D. Ciceron, F. Garcia, Nanofiltration membranes for drinking water production - retention of nitrate ions, Desalin. Water Treat. 57 (2016) 16758–16769.

[30] R. Epsztein, O. Nir, O. Lahav, M. Green, Selective nitrate removal from groundwater using a hybrid nanofiltration–reverse osmosis filtration scheme, Chem. Eng. J. 279 (2015) 372–378. doi:10.1016/j.cej.2015.05.010.

[31] D.-X. Wang, M. Su, Z.-Y. Yu, X.-L. Wang, M. Ando, T. Shintani, Separation performance of a nanofiltration membrane influenced by species and concentration of ions, Desalination. 175 (2005) 219–225. doi:10.1016/j.desal.2004.10.009.

[32] K. Häyrynen, E. Pongrácz, V. Väisänen, N. Pap, M. Mänttäri, J. Langwaldt, et al., Concentration of ammonium and nitrate from mine water by reverse osmosis and nanofiltration, Desalination. 240 (2009) 280–289. doi:10.1016/j.desal.2008.02.027.

[33] L.A. Richards, M. Vuachère, A.I. Schäfer, Impact of pH on the removal of fluoride, nitrate and boron by nanofiltration/reverse osmosis, Desalination. 261 (2010) 331–337. doi:10.1016/j.desal.2010.06.025.

[34] A. Santafé-Moros, J.M. Gozálvez-Zafrilla, J. Lora-García, Nitrate removal from ternary ionic solutions by a tight nanofiltration membrane, Desalination. 204 (2007) 63–71. doi: 10.1016/j.desal.2006.04.024

[35] W.R. Bowen, J.S. Welfoot, Modelling the performance of membrane nanofiltration - critical assessment and model development, Chem. Eng. Sci. 57 (2002) 1121–1137. doi:10.1016/S0009-2509(01)00413-4.

[36] D. Chen, X. Zhao, F. Li, Treatment of low level radioactive wastewater by means of NF process, Nucl. Eng. Des. 278 (2014) 249–254. doi:10.1016/j.nucengdes.2014.08.001.

[37] M.A. Sari, S. Chellam, Relative contributions of organic and inorganic fouling during nanofiltration of inland brackish surface water, J. Memb. Sci. 523 (2017) 68–76. doi:10.1016/j.memsci.2016.10.005.

[38] A.O. Aguiar, L.H. Andrade, B.C. Ricci, W.L. Pires, G.A. Miranda, M.C.S. Amaral, Gold acid mine drainage treatment by membrane separation processes: An evaluation of the main operational conditions, Sep. Purif. Technol. 170 (2016) 360–369. doi:10.1016/j.seppur.2016.07.003.

[39] J.A. Redondo, F. Lanari, Membrane selection and design considerations for meeting European potable water requirements based on different feedwater conditions, Desalination. 113 (1997) 309–323. doi:10.1016/S0011-9164(97)00147-1.

[40] C. Bellona, J.E. Drewes, The role of membrane surface charge and solute physico-chemical properties in the rejection of organic acids by NF membranes, J. Memb. Sci. 249 (2005) 227–234. doi:10.1016/j.memsci.2004.09.041.

[41] J.V. Nicolini, C.P. Borges, H.C. Ferraz, Selective rejection of ions and correlation with surface properties of nanofiltration membranes, Sep. Purif. Technol. 171 (2016) 238–247. doi:10.1016/j.seppur.2016.07.042.

[42] E. Chilyumova, J. Thöming, Nanofiltration of bivalent nickel cations — model parameter determination and process simulation, Desalination. 224 (2008) 12–17. doi:10.1016/j.desal.2007.04.072.

[43] C.Y. Tang, Y.-N. Kwon, J.O. Leckie, Characterization of Humic Acid Fouled Reverse Osmosis and Nanofiltration Membranes by Transmission Electron Microscopy and Streaming Potential Measurements, Environ. Sci. Technol. 41 (2007) 942–949. doi:10.1021/es061322r.

[44] L. Llenas, G. Ribera, X. Martínez-Lladó, M. Rovira, J. de Pablo, Selection of

nanofiltration membranes as pretreatment for scaling prevention in SWRO using real seawater, Desalin. Water Treat. 51 (2013) 930–935. doi:10.1080/19443994.2012.714578.

[45] P. Xu, J.E. Drewes, D. Heil, Beneficial use of co-produced water through membrane treatment: technical-economic assessment, Desalination. 225 (2008) 139–155. doi:10.1016/j.desal.2007.04.093.

[46] M. Tahaikt, R. El Habbani, A. Ait Haddou, I. Achary, Z. Amor, M. Taky, A. Alami, A. Boughriba, M. Hafsi, A. Elmidaoui, Fluoride removal from groundwater by nanofiltration, Desalination. 212 (2007) 46–53. doi:10.1016/j.desal.2006.10.003.

[47] L. Paugam, C.K. Diawara, J.P. Schlumpf, P. Jaouen, F. Quéméneur, Transfer of monovalent anions and nitrates especially through nanofiltration membranes in brackish water conditions, Sep. Purif. Technol. 40 (2004) 237–242. doi:10.1016/j.seppur.2004.02.012.

[48] J.J. Qin, M.H. Oo, H. Lee, B. Coniglio, Effect of feed pH on permeate pH and ion rejection under acidic conditions in NF process, J. Memb. Sci. 232 (2004) 153–159. doi:10.1016/j.memsci.2003.12.010.